



# Design of Enhanced Smart Delivery Systems for Therapeutic Enzymes: Kinetic and Release Performance of Dual Effectuated Enzyme-Loaded Nanopolymers

Ömür Acet<sup>1</sup>

Received: 15 May 2023 / Accepted: 10 July 2023 / Published online: 20 July 2023

© The Author(s), under exclusive licence to Springer Science+Business Media, LLC, part of Springer Nature 2023

## Abstract

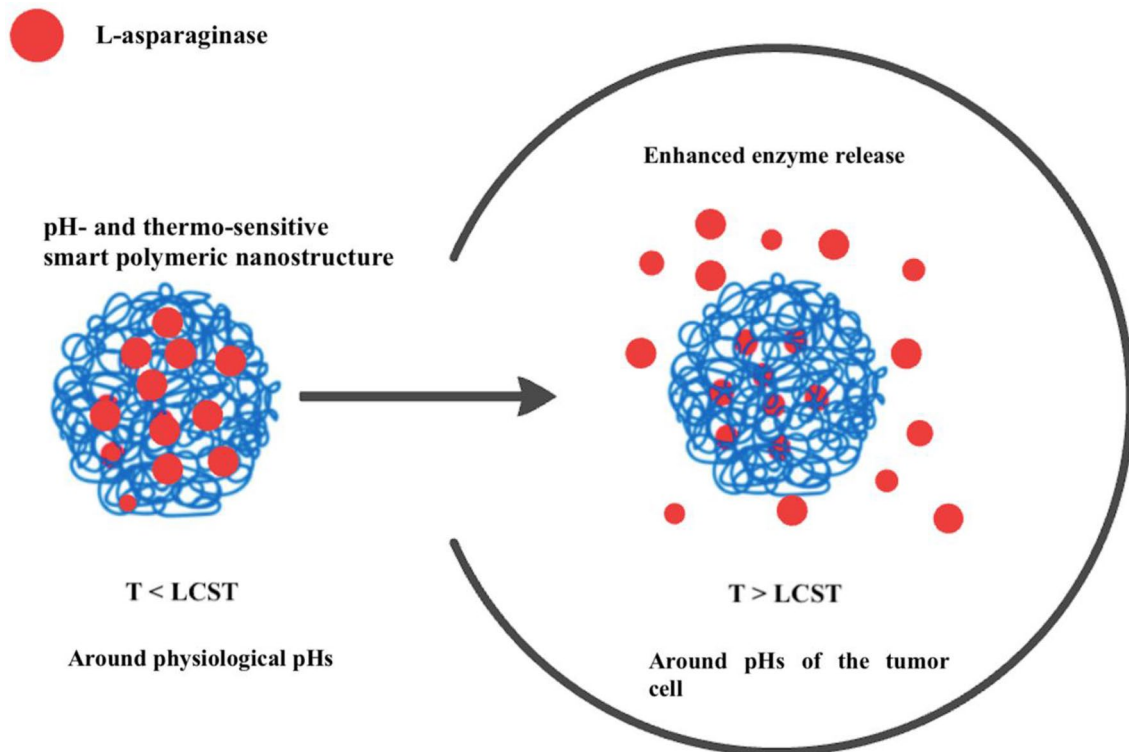
L-asparaginase (L-ASNase) is among the important biopharmaceuticals and is utilized in the treatment of acute lymphoblastic. L-ASNase catalyzes its conversion to aspartic acid and ammonia. The use of enzymes loaded on polymeric systems is an alternative way to avoid the stability problem when using enzymes. In addition, drug release applications that can be obtained with loaded enzymes can be very useful, especially in both pharmaceutical and medical implementations, as they can canalize the enzyme to the right site. For this purpose, L-asparaginase loaded smart nanopolymers (ASN-SNPs) were synthesized via miniemulsion process. The SEM, FTIR characterizations and, zeta potential of ASN-SNPs were carried out. ASN-SNPs showed improvement in free enzyme related stability under extreme conditions. On the other hand, the storage stability and reusability of theASN-SNPs were found to be about 63 and 53% of the original activity after 4 weeks days at room temperature and 10 cycles, respectively. The Michaelis–Menten constants ( $K_m$ ) of 6.595 and 1.902 mM, and the maximum reaction rates ( $V_{max}$ ) of 212.766 and 49.02  $\mu\text{M min}^{-1}$  were founded for free and loaded L-ASNase, respectively. The results showed that the designed L-asparaginase loaded SNPs are a promising matrix for their high catalytic efficiency and enhanced stability properties.

---

✉ Ömür Acet  
omuracet@tarsus.edu.tr

<sup>1</sup> Pharmacy Services Program, Vocational School of Health Science, Tarsus University, Tarsus, Turkey

## Graphical Abstract



**Keywords** L-asparaginase · Enzyme activity · Smart nanoparticles · Temperature · pH sensitive nanopolymer

## 1 Introduction

L-asparaginase (L-ASNase), an amidohydrolase that catalyzes the conversion of L-asparagine (L-Asn) to aspartic acid and ammonia, is among the most important biopharmaceuticals. L-ASNase has been used around the world as a therapeutic agent for the treatment of Acute Lymphoblastic Leukemia (ALL) [1]. Leukemia cells can not increase in numbers with the presence of L-ASNase enzyme as a result of this event leukemia cells die. The chemotherapeutic efficacy of the L-ASNase is associated with this fact [2]. L-ASNase also accounts for approximately 40% of the total enzyme market in healthcare has a high and constantly demanding global market [1, 3]. On the other hand, the recent commercialization of fungal L-ASNases in the food industry to hinder acrylamide formation has attracted great interest [1].

Although enzymes are biological catalysts that make easy complex chemical reactions at optimum circumstances, they are influenced by several special conditions (e.g., pH and temperature) [4, 5]. New designs that will behave according to environmental conditions such as pH and temperature and increase the activities of enzymes

can be extremely beneficial. Synthetic polymers display easily tailored features, which makes possible their adaptation to several applications. In addition, they exhibit an inert behavior at physiological mediums. Polymers with synthetic structure can offer mechanical/chemical stability and good reproducibility [6].

In the process of entrapping an enzyme in a polymer network, it traps the enzyme while allowing substrates and products to pass through. In addition, under certain conditions, a controlled release of the enzyme to the target site may also occur [7]. Thus, the enzyme molecules do not interact with the polymer in any way, minimizing the active site block problems experienced by adsorption methods that are mostly used for industrial applications [8, 9].

Many methods have been studied and investigations are still ongoing to obtain durable and highly active biocatalysts. In these studies, polymers clearly play an important role. The utilization of some polymers (such as synthetic, natural, inorganic and smart polymers) has been reported in the literature to date [9]. Nowadays, polymeric nanoparticles have appeared as highly up-and-coming and feasible platforms for targeted and controlled drug delivery [10].

The creation of biopharmaceutical agents with improved quality is one of the most important guiding principles of the “Quality by Design” paradigm. This principle includes not only the clinical status the new product is presumed to treat, but also its pharmacokinetics, pharmacodynamics and potential toxicity [11–13]. Therefore, both effective and non-toxic designs are extremely important. “Stimulus sensitive” polymers, also called “smart” polymers, are attracting increasing concern these days due to their talent to consist conformational changings or show phase transitions behaviour in response to external stimuli [14]. Different “smart” polymeric nanoparticle platforms that may respond through drug release against an internal/external stimulants (i.e., pH, redox, temperature, magnetic and light) have been reported in the literature. Such smart systems are known to have significant improvements in in vitro/in vivo drug release performance despite varying drug loading levels [15]. In addition, studies have displayed that the response of polymeric nano-platforms to binary/multiple systems can better enhance drug delivery capacity compared to nano-platform systems that respond to a single stimulus [10, 16].

Enzyme entrapment can be highly beneficial in both pharmaceutical and medical applications, especially in drug release applications, as they may canalize the enzyme to the right site. Researchers face a major stability problem when using enzymes. Enzymes can easily become unstable due to environmental parameters (such as changes in temperature, pH, or ionic strength). Thus, entrapment platforms with polymers are another way of preserving the catalytic activity of enzymes and their stability in reaching the target site of release or during usage in a reaction [9].

The subtle differences between body and room temperature and the pH difference between the environment and the target site are the main reasons why heat and pH sensitive polymers are a crucial class of smart materials for drug delivery. Especially, the responsive polymeric platforms should be stable at physiological pH for such implementations [14]. PNIPAM is the most well-known and researched thermosensitive polymer [10, 14] and is commonly used in, but not restricted to, controlled drug release studies [17–19]. Its use is not limited to these studies as the low critical solution temperature is close to body temperature as its lower critical solution temperature (LCST) (32 °C) is close to the temperature of body [14]. Vinyl imidazole (VIm) is a pH sensitive chemical agent [20] and the event of deprotonation of VIm around physiological pH may offer advantage for drug delivery systems, especially for the project of pH sensitive polymers [21]. The pH value of normal tissues and blood (pH: 7.4) is higher than the pH (pH: 6.5–6.8) of tumor cell endosomes and lysosomes. Dual sensitive systems (pH and thermo sensitive) can be designed to generate preferable targeting and low systemic side effects [22, 23].

Here, L-ASNase loaded temperature and pH sensitive smart nanopolymers (ASN-SNPs) were produced. Smart nanopolymers were characterized with Fourier transform infrared spectrophotometer (FTIR), scanning electron microscopy (SEM), zeta potential analysis. The L-ASNase loading capacity of the synthesized smart nanopolymers was investigated, as well as the effects on L-ASNase release over time to examine the release behavior of different environmental conditions against pH and temperature change. ASN-SNPs showed improved in the stability in connection with the free enzyme at extraordinary circumstances around acidic pH and high temperature. Additionally, the storage stability and reusability of ASN-SNPs were determined 63 and 53% of the original activity after 4 weeks days at room temperature and 10 cycles, respectively. The Michaelis–Menten constants ( $K_m$ ) of 6.595 and 1.902 mM, and the maximum reaction rates ( $V_{max}$ ) of 212.766 and 49.02  $\mu\text{M min}^{-1}$  were founded for free and ASN-SNPs, respectively. The activity results obtained were found to be comparable with the studies in the literature [2, 3, 24, 25]. These results proved that SNPs are good carrier matrix with high catalytic efficiency and enhanced stability.

## 2 Materials and Methods

### 2.1 Materials

L-ASNase isolated from *E. coli*, Leunase, Japan was used in the enzymatic activity measurements. Other chemicals utilized in this assay were purchased from Sigma (St. Louis, MO, USA). Water utilized in study was purified by utilizing a Barnstead (Dubuque, IA, USA) ROpure LP® reverse osmosis unit.

### 2.2 Methods

#### 2.2.1 Synthesis of the ASN-SNPs

Miniemulsion polymerization technique was used to synthesize L-ASNase loaded nanopolymers. In summary, it is as follows: The first water phase was formed. This phase was formed by dissolving a mixture of Polyvinyl alcohol (PVA, 0.375 g), sodium dodecyl sulfate (SDS, 57.7 mg) and sodium bicarbonate ( $\text{NaHCO}_3$ , 46.9 mg) in 20 mL of water. Secondly, the dispersion phase, called the water phase, was made ready by dissolving PVA (0.2 g) and SDS (0.2 g) in 400 mL of water). The organic phase was 2-hydroxyethyl methacrylate (HEMA, 0.8 mL), ethylene glycol dimethacrylate (4.2 mL, EGDMA), N-isopropylacrylamide (NIPA, 400 mg), vinylimidazole (1.5 mL, VIm), acrylamide (100 mg, AAm). The prepared organic phase was mixed and provided for 30 min until the components were completely

dissolved. Then, it was united to the first prepared water phase and miniemulsions were taken place for 5 min with the help of a homogenizer (T25B, Ika Labortechnik, Germany). Then, the second water phase was taken into a 1 L 2-necked flask and mixed until the temperature was 50 °C by means of a mechanical mixer. Then the first prepared water phase, the mixture consisting of the organic phase was added to the second water phase and mixed with a mechanical mixer at 50 °C. It was mixed at 500 rpm rotation speed. Lastly, ammonium persulfate (APS, 0.252 g) and sodium bisulfite (NaHSO<sub>3</sub>, 0.230 g) redox initiator pair were put into the medium to initiate the polymerization. The polymers formed by the polymerization process for 10 h, the surfactants and unreacted monomers were eliminated by washing with solution (ethanol–water mixture) and centrifuged at 25,000 rpm (Beckman Coulter, Allegra 64R Centrifugen, USA). The precipitated nanopolymer was dispersed back into distilled water by using a sonicator and dried with the help of a lyophilizer. 10 mg of lyophilized nanopolymers and 5 enzyme unit were dispersed in phosphate buffer solution (PBS) and the solution was stirred for 3 days at 24 °C to allow L-ASNase to be retained within the nanoparticle network. After 3 days of incubation period, the nanopolymer solution was washed with PBS for 3 h to remove free L-ASNase (this time was predetermined for optimal separation of loaded L-ASNase). Then, these nanopolymers were stored at 4 °C.

### 2.2.2 Characterizations of SNPs

The morphology and shapes of SNPs were screened by Scanning electron microscopy (SEM) (Leo 440 computer controlled digital) by using lyophilized SNPs. FTIR spectra of ASN-SNPs and L-ASNase were obtained via FTIR spectrophotometer and wavelength range of 650–4000 cm<sup>-1</sup> with a resolution of 2 cm<sup>-1</sup> (Perkin Elmer, 400, FTIR spectrophotometer). Zeta potential of ASN-SNPs in 0.1 M PBS buffer with a pH of 7.0 (0.5 mg/mL) was made decision by utilizing Nano Zetasizer (NanoS, Malvern Instruments, London, England).

### 2.2.3 L-ASNase Loading and Releasing Studies

At this stage, the loading capacity of SNPs for L-ASNase was carried out with concentration ranges of 0–50 enzyme unit (10 mg SNPs in 10 mL of 0.05 M phosphate buffer, pH 7.4, 24 °C). The change of enzyme concentration in the solution during and after loading enzyme in medium was measured by means of a UV/Vis spectrophotometer at 280 nm (Shimadzu, Tokyo, Japan, Model 1601). Enzyme loading was carried out with this method in experiments at other stages. In the release studies of ASN-SNPs, the release behavior of the pH and temperature parameters was

observed in different ambient conditions by using 5 enzyme unit concentrations.

### 2.2.4 Determination of L-ASNase Activity

L-ASNase activity was determined spectrophotometrically by the Nesslerization method [26]. L-ASNase enzyme hydrolysis L-asparagine (L-Asn) amino acid to L-aspartic acid (L-Asp) and ammonia. This method is widely used based on the measurement of ammonia released as a result of the breakdown of L-asparagine by added Nessler reagent. Free and loaded L-ASNase were taken and incubated for 15 min at 37 °C with a freshly prepared L-asparagine substrate solution (10 mM, 1 mL) in Tris–HCl (50 mM, pH: 8.6) buffer. Then the reaction was stopped by adding trichloroacetic acid (1.5 M, 0.1 mL). Afterwards, 0.1 mL of Nessler reagent was added to 0.1 mL, afterword the absorbance was measured at 480 nm Each measurement was repeated triplicate and the average was taken. One unit of enzyme activity (U) was described as the amount of L-ASNase necessary to liberate 1 μmol of ammonia per minute.

### 2.2.5 Yield and Efficiency of L-ASNase Loaded

The loaded yield (*LY*) and loaded efficiency (*LE*) were calculated by using the equations below:

$$LY(\%) = \frac{C_i - C_s}{C_i} * 100$$

where, while *C<sub>i</sub>* presents the total protein concentration of the enzyme, *C<sub>s</sub>* shows the total protein concentration of the unbound enzyme in the supernatant and washing solutions.

$$LE(\%) = \frac{A_i}{A_f} * 100$$

As for loaded efficiency, here, *A<sub>i</sub>* and *A<sub>f</sub>* express the activity of the ASN-SNPs and the free L-ASNase, respectively.

### 2.2.6 Effect of pH and Temperature

The effect of pH was tested by measuring the activity of free and ASN-SNPs at different pH buffers, L-Asn substrate dissolved in different pH buffers, ranging from pH 5.0–10.0. The buffers used in this assay were sodium acetate (pH 5.0–6.0), PBS (pH 7.0–8.0), and Tris–HCl (pH 9.0–10.0). As well as the effect of temperature on the free and ASN-SNPs were investigated by determining the enzyme activity at various temperatures ranging from 30 to 70 °C. The maximum activity was confirmed as 100% and the outcomes were converted to relative activities. The data with the maximum activity was made decision as the optimum value.



### 2.2.7 Thermal and Storage Stability

To examine the thermal stability of the ASN-SNPs, free and ASN-SNPs were incubated at 50 °C at various times (from 0 to 180 min). At the end of each incubation period, a routine enzyme assay was followed to determine residual enzyme activity. The activity observed for 0 min was taken as control 100%.

The storage stabilities of the ASN-SNPs and free L-ASNase enzymes were examined by storing at 25 °C for four weeks. The enzyme activity was evaluated on the first day and considered as control 100%, and subsequent activities were transformed to relative activity.

### 2.2.8 Reusability

To determine the reusability of the ASN-SNPs, the activity was measured under optimum conditions. After each activity measurement, the ASN-SNPs were separate from the supernatant then the activity was measured by the Nessler reagent. Thereafter, the activity was restarted by adding a fresh substrate to the ASN-SNPs. The first measured enzyme activity was accepted as 100% and this process was repeated for 10 successive reuses.

### 2.2.9 Kinetics ( $K_m$ and $V_{max}$ )

To estimate the kinetic parameters ( $K_m$  and  $V_{max}$ ), the activity of the free L-ASNase and ASN-SNPs were measured at different substrate L-Asn concentrations under standard

assay conditions.  $K_m$  and  $V_{max}$  values were estimated via the Lineweaver Burk plot.

## 3 Results and Discussion

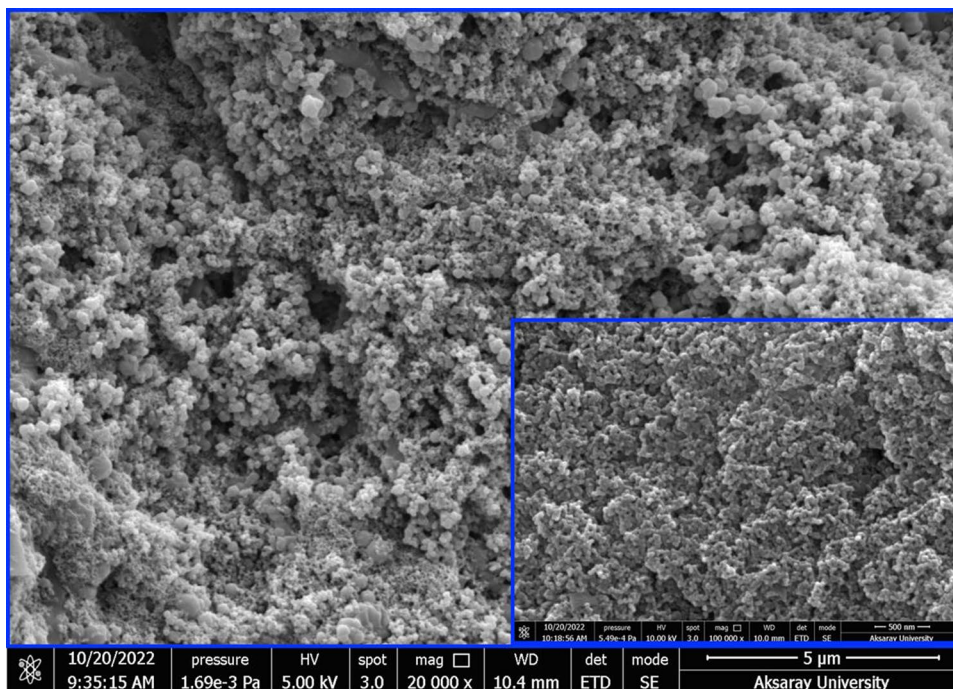
### 3.1 Characterizations

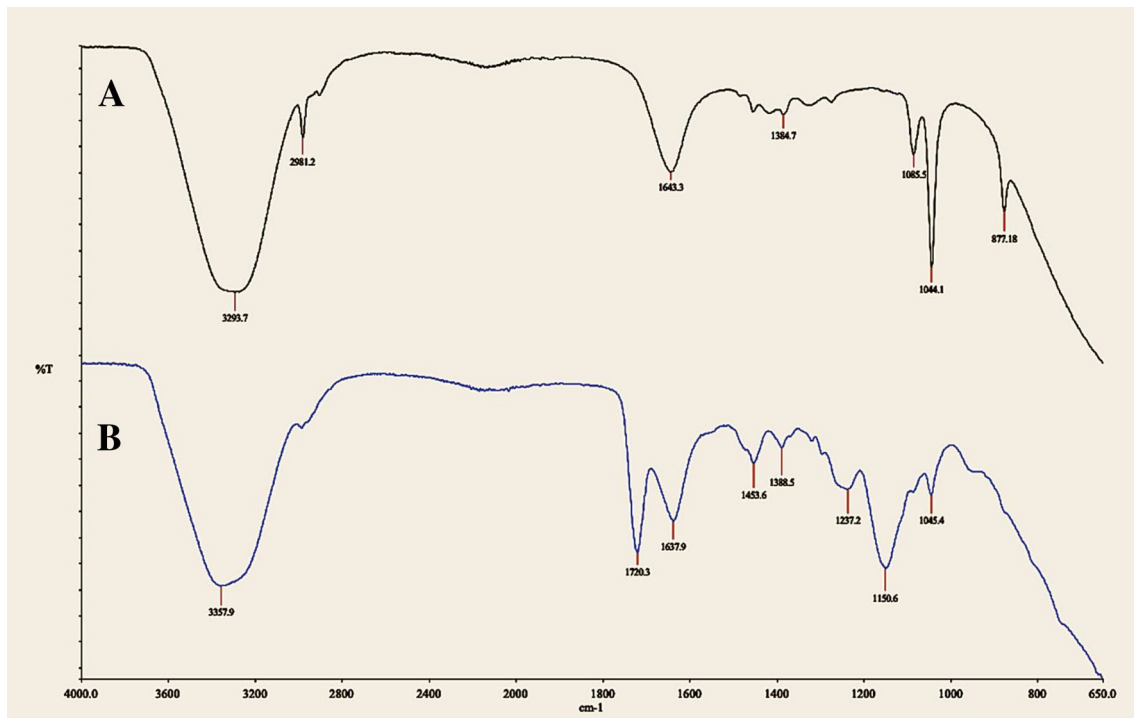
The structure and the surface morphology of the smart nanoparticles are demonstrated in Fig. 1. As seen here, the synthesized SNPs were spherical in shapes. Even though SNPs are nanostructures around 250 nm at a low level, the majority of the synthesized structures are 150 nm nanostructures. In particular, these sizes will provide a significant advantage to the nanoparticles synthesized in intracellular uptake.

Figure 2 demonstrates FTIR spectra of SNPs and ASN-SNPs. The spectra shows that the broad peak about  $3300\text{ cm}^{-1}$  was due to stretching of  $-\text{OH}$  and  $\text{N}-\text{H}$  groups. And also,  $\text{C}-\text{H}$  stretching and  $\text{C}-\text{O}$  stretching vibrations bands were seen at around  $2981\text{ cm}^{-1}$  and  $1300\text{ cm}^{-1}$ , respectively. A peak at  $1643\text{ cm}^{-1}$  assigned as stretching vibration of  $\text{C}=\text{O}$  group. After enzyme loading, the FTIR spectrum of ASN-SNPs showed two new peaks at  $1720$  and  $1637\text{ cm}^{-1}$ , which may be ascribed to amide I (the vibration of the  $\text{C}=\text{O}$  bonds) and amide II (a combination of  $\text{C}-\text{N}$  stretching and  $\text{N}-\text{H}$  vibration in protein backbone), respectively [3]. These results showed that L-ASNase was loaded into SNPs in a successful way.

Nanoparticles could display a high affinity demand to the cell membrane with electrostatic interactions [27].

**Fig. 1** SEM images of smart nanoparticles in different sizes





**Fig. 2** FTIR spectra of (A) smart nanoparticles and (B) L-asparaginase loaded smart nanoparticles

Cell membranes have large negative charges necessary to repel negatively charged nanostructures [28]. The zeta potential of ASN-SNPs was measured as +14.1 mV at pH 7.0. Positively charged nanostructures are preferentially taken up by tumors [29, 30] and are retained for a longer period of time than negatively or neutrally charged structures [30]. This value reveals the potential of using ASN-SNPs for biomedicine applications.

### 3.2 Loading of L-ASNase into SNPs

As seen in Fig. 3A L-ASNase capacity increased, correlating with the increase in concentration. It has reached its maximum in 50 enzyme unit (636.2 mg/g polymer). High loading performance of L-ASNase at low concentrations came about quickly owing to the high surface area of SNPs. SNPs achieved a high loading performance even at low concentration of L-ASNase molecules because of rapid filling of their adsorption fields.

The study was carried out by investigating the effects of pH and temperature on the release behavior of L-ASNase

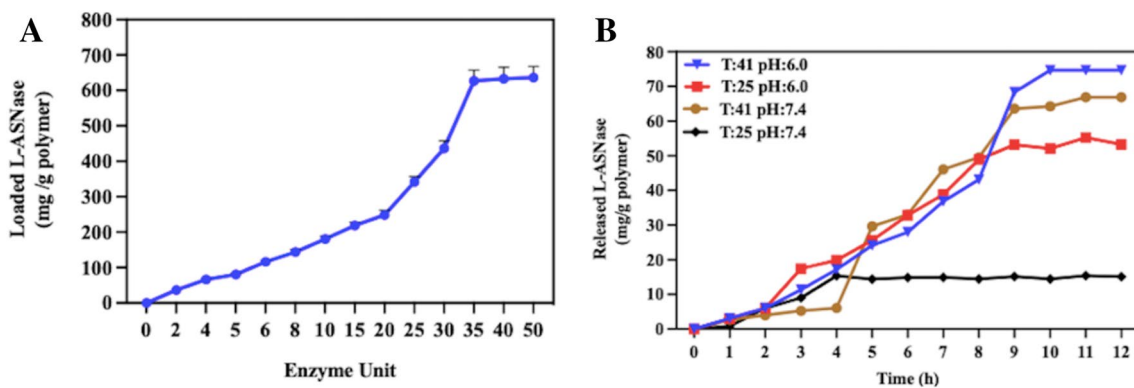


**Fig. 3** A Loading capacity of L-ASNase smart nanoparticles. B The effect of pH and temperature parameters on L-ASNase release after 12 h

loaded smart nanopolymeric structures, and the release amount after 12 h (Fig. 3B). As shown in Fig. 3B, it presented a remarkable effect on the nanopolymeric release profile at both pH 6.0 and 41 °C. L-ASNase release is very low for experimental studies where there is no effect. Due to the deprotonation of vinyl imidazole around cell pH, L-ASNase loaded nanostructures caused enzyme release, and thus the synthesized polymer fulfilled its pH-sensitive task. On the other hand, as the polymer begins to rise above the LCST (from 25 to 41 °C), the structure of polymer expanded and greatly conducted to the enzyme release. Thermo-sensitive nanostructures are in a shrunken form at physiological temperature above the LCST value. Enzyme loading happens at temperatures lower than the LCST value, while L-ASNase loaded on nanostructures is released in smart nanostructures as temperatures above the LCST value. The results obtained showed that the highest burst release behavior with the dual effect of temperature and pH. This study also demonstrated that the response of binary/multiple smart nanosystems may better improve drug delivery performance as per to nanosystems that respond to a single stimulus.

### 3.3 Yield and Efficiency of L-ASNase Loaded

The loading yield (*LY*) and loading efficiency (*LE*) of ASN-SNPs were calculated as  $78.68 \pm 2.47\%$  and  $74.67 \pm 3.56\%$ , respectively. These results revealed that L-ASNase was successfully loaded onto smart nanopolymers.

### 3.4 Effect of pH and Temperature on L-ASNase Activity

The activity with varying pH is a major parameter in the applications of enzyme loading. The activities of the free and loaded L-ASNase were studied at different pH domains

from 5.0 to 10.0. According to observed data (Fig. 4A), the maximal activity of the ASN-SNPs was found at pH 7.0, while free L-ASNase was found to be at pH 8.0. However, the residual activity of free L-ASNase and ASN-SNPs started to decrease above pH 8.0. The ASN-SNPs showed good pH stability in an alkaline environment the relative activity has remained above 79% for ASN-SNPs and more than 64% for free L-ASNase at pH 10.0. Noma et al. determined the optimum pH of free and immobilized L-ASNase change from pH 7.5 to 8.5. [31]. Similarly, in another study, the optimum pH of free and immobilized L-ASNase was shifted from pH 7.0 to 9.0 [32]. The possible reason for this slight shift in pH may be because of variations in support materials that were used. It is observed that ASN-SNPs exhibited high relative activity in the pH ranges from 5.0 to 10.0. This excellent performance of the ASN-SNPs could be due to the interactions between the L-ASNase and the SNPs. In addition, compared to the free enzyme, the activity of the ASN-SNPs was generally higher across the majority of pH ranges. According to the pH stability tests, the loaded L-ASNase was marginally more stable than the free enzyme. The higher pH stability has advantageous for the ASN-SNPs to be used in the medical application.

The enzyme activity at various temperatures is one of the important parameters for enzyme studies. Therefore, the enzyme activities for the free and ASN-SNPs were measured at various temperatures in order to examine if there is a change in the optimum temperature after loading process. The optimum temperature of free L-ASNase and ASN-SNPs were measured to be 40 and 45 °C, respectively as shown in (Fig. 4B). In addition, the ASN-SNPs maintained more than 73% and free L-ASNase maintained nearly 55% of their activity at 60 °C, then the relative activity of free L-ASNase was only 38% while ASN-SNPs was 52% at 70 °C. The results indicated that the smart nanopolymers have protected

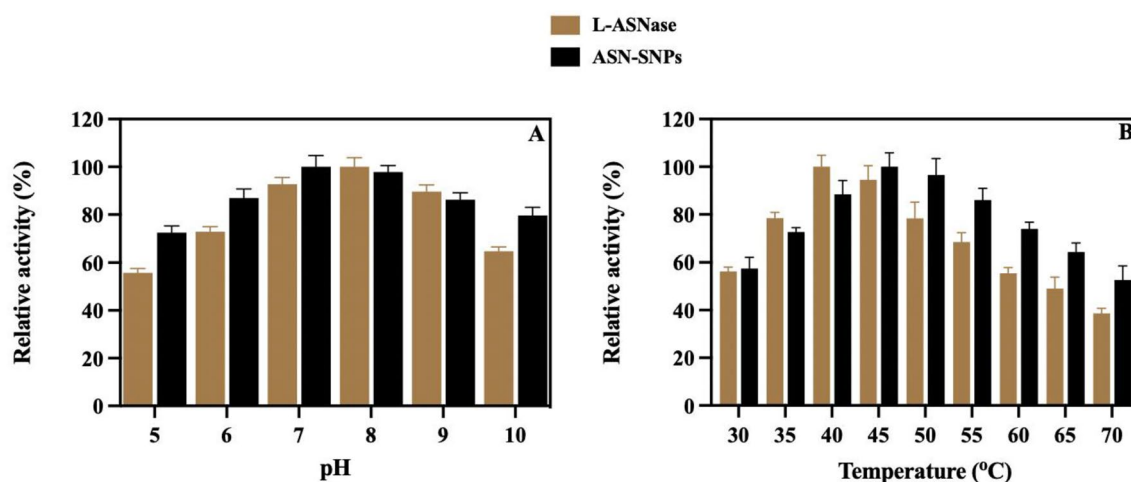


Fig. 4 The effect of different A pH and B temperature values on the activity of free and L-asparaginase loaded smart nanopolymers

the enzyme from inappropriate changes at high temperatures. In prior investigations, a similar outcome of optimum temperature for immobilized L-ASNase and very close result for free L-ASNase has been observed [32]. However, depending on the type of interaction between the enzyme and the matrix as well as the matrix, the extent of displacement differed. As a result of the intermolecular connections that form between the enzyme molecules and the matrix support, the structure of the enzyme molecule is made stiff and is therefore less susceptible to the denaturing effects of temperature [33].

### 3.5 Thermal and Storage Stability of L-ASNase

The thermal stability study of free and ASN-SNPs was carried out by incubation at temperature degrees above their optimum temperatures that were founded. Both enzymes were incubated at 50 °C, then the activities were measured at different interval times (0, 5, 10, 15, 30, 60, 120, and 180 min) as shown in (Fig. 5A). The free L-ASNase and ASN-SNPs showed above that 87 and 94% from the relative activity after incubation for 15 min of at 50 °C. Furthermore, after 60 min of incubation, the free and ASN-SNPs preserved more than 61 and 81% of their initial activities, respectively, while at the end of 180 min free L-ASNase and ASN-SNPs preserved 32 and 55% of their original activity at 50 °C. These findings revealed that the smart nanoparticles provide a suitable microenvironment for ASN-SNPs and provide protection against environmental factors such as high temperature that may reduce the activity. In accordance with loading, L-ASNase was loaded to SNPs, which inhibited change in conformation and reduced molecular mobility due to attraction forces between the enzyme and

carrier matrix. Overall, the thermal stability of L-ASNase enhanced after loading on SNPs.

One of the most important advantages of enzyme studies is storage stability, it is an urgent need in industrial areas to have better storage stability as per to free enzymes. The storage stability of the free and ASN-SNPs was determined by measuring activities of both at every single week for 4 weeks at 25 °C. As seen in (Fig. 5B), at the end of the first week the retained enzyme activity for free L-ASNase and ASN-SNPs was 87 and 93%, respectively of initial activities. Nevertheless, the activity was still above 42 and 63% for free and immobilized L-ASNase, respectively at the end of the fourth week. A significant improvement in the enzyme activity after loading to smart nanoparticles was observed with increasing storage time. The satisfactory ability of the smart nanoparticles in long-term storage was owing to multiple linkages between the L-ASNase and the smart nanoparticles present, which prevented enzyme denaturation or leaching from the support. As a result, it is acceptable to conclude that the ASN-SNPs displayed enhanced storage stability.

### 3.6 Reusability

The reusability of loaded L-ASNase is the key to cost-effectiveness for medical and industrial applications. The reusability of the ASN-SNPs was investigated by hydrolyzing of L-Asn for 10 consecutive cycles. The residual activity was found to be 92.3% after 3 cycles, 83.2% after 5 cycles, 70.3% after 7 cycles, and even after 10 cycles, the residual activity was still above 53% from the initial activity as shown in Fig. 6. The relative activity of the ASN-SNPs gradually decreased through the reaction cycles between L-ASNase and SNPs because of leaching from the SNPs matrix. In addition to that, L-ASNase activity was maintained above

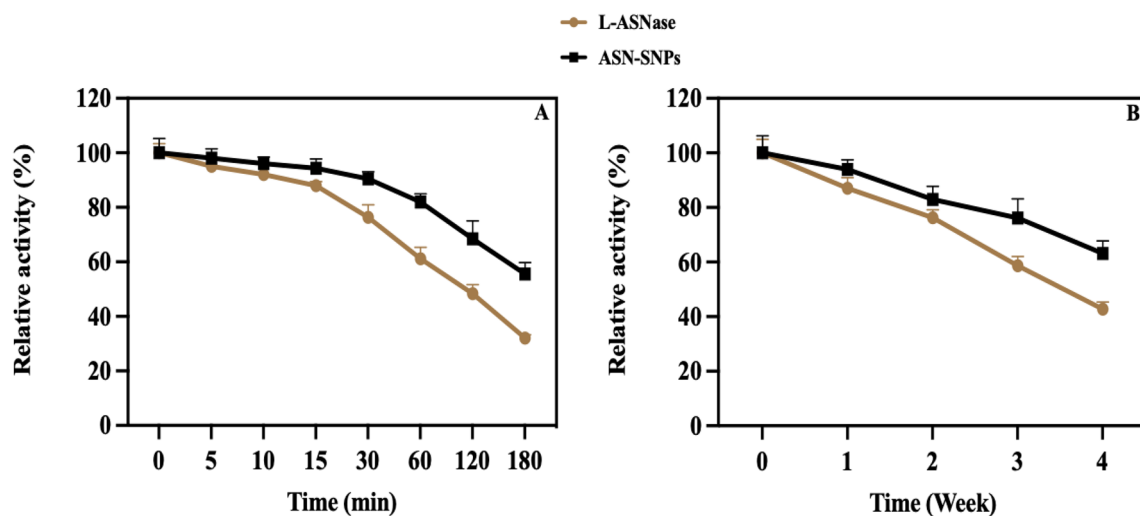
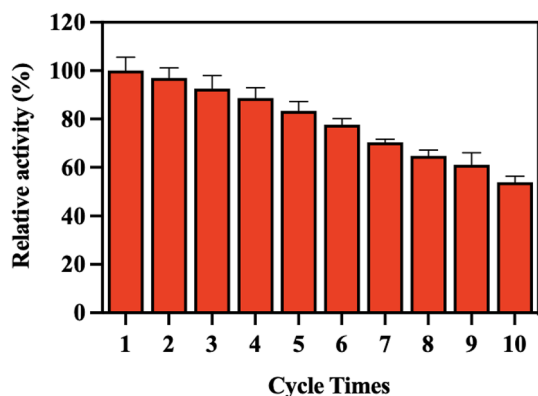


Fig. 5 **A** Thermal stability, **B** storage stability of free and L-asparaginase loaded smart nanoparticles





**Fig. 6** The reusability of L-asparaginase loaded smart nanoparticles by using L-Asn as substrate

half of the initial activity up to 10 reuse cycles, it can be considered that a highly stable biocatalyst is obtained by the loading of L-ASNase to SNPs. And because of that, ASN-SNPs appears to be much more reusable than their counterparts reported in the literature using other support. For instance, the immobilized L-ASNase on graphene oxide and graphene oxide carbonyldiimidazole support matrix the relative activities were still around 29 and 42% of initial activities after 8 cycles [34], about 70% of residual activity was obtained after 5 cycles for L-asparaginase on magnetic nanoparticles [35]. Compared to these findings, loading L-ASNase into SNPs could promising and bring a chance for

L-ASNase to be used in medical and industrial application and as biocatalysts in continuous reactors.

### 3.7 Kinetics $K_m$ and $V_{max}$

The values of  $K_m$  and  $V_{max}$  from the Lineweaver–Burk plot were given in (Fig. 7). The relation between substrate concentration and reaction rate of free and immobilized L-ASNase were determined by different concentrations of L-Asn substrate at the optimum condition of enzyme activity assay. The  $K_m$  value of the ASN-SNPs was 1.902 mM which was lower than the free L-ASNase 6.595 mM. This outcome means that the enzyme on the surface of ASN-SNPs has more accessible potential active sites, thus increasing the affinity of the L-ASNase to the L-Asn substrate. In contrast, the  $V_{max}$  of the ASN-SNPs was  $49.02 \mu\text{M min}^{-1}$ , which was lower than that of the free L-ASNase  $212.766 \mu\text{M min}^{-1}$ .

The decrease in  $V_{max}$  of the ASN-SNPs is because of the difficulty to reach the enzyme after immobilization that due to SNPs can make a hindrance to enzyme reaching the substrate. A study was reported for immobilized L-ASNase magnetic  $\text{Fe}_3\text{O}_4@\text{MCM-41}$  core–shell nanoparticles, according to the results of L-ASNase enzyme increased in  $V_{max}$  value from  $288 \pm 12.5$  to  $909 \pm 23.4$  U/mg protein, and decrease in  $K_m$  concentration from  $0.052 \pm 0.006$  to  $0.045 \pm 0.007$  mM after immobilization [36]. In another study, chloro-modified magnetic  $\text{Fe}_3\text{O}_4@\text{MCM-41}$  core–shell nanoparticles for L-Asparaginase immobilization

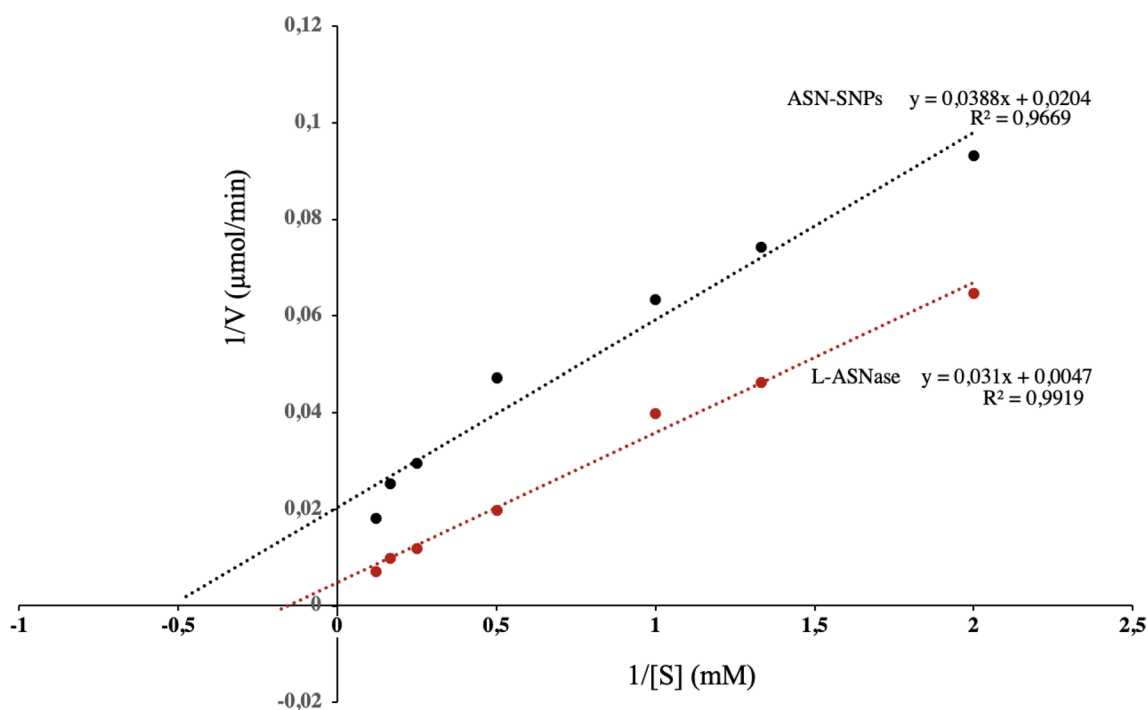


**Fig. 7** The Lineweaver–Burk plot of free and L-asparaginase loaded smart nanoparticles

they obtained the  $K_m$  and  $V_{max}$  values  $65 \pm 0.078$  mM and  $32.2 \pm 4.37$   $\mu\text{M min}^{-1}$  for free L-ASNase and  $0.62 \pm 0.086$  mM and  $11.81 \pm 0.78$   $\mu\text{M min}^{-1}$  for immobilization of L-ASNase, respectively [25]. According to reports, the main factor causing lower  $K_m$  could be immobilization, which prevents conformational change and results in limited substrate diffusion.

## 4 Conclusion

Maintaining their stability when using enzymes is a huge problem. The stability of enzymes is at risk of becoming unstable under adverse environmental conditions such as temperature and pH. Thus, delivery methods used by encapsulation or loading into polymers are an alternative way of maintaining the catalytic activity of enzymes until they reach the target site where they are released or are used in a reaction where they are to be used. L-ASNase loaded temperature and pH sensitive smart nanoparticles were synthesized and characterizations conducted with SEM and FTIR analyses. The highest L-ASNase loading capacity to SNPs was 636.2 mg/g polymer at pH: 7.4, 24 °C. The maximum release of L-ASNase was observed in the dual effect operating environment of the smart polymer as designed (T: 41 °C, pH 6.0). ASN-SNPs demonstrated wider range of work pH and temperature range and improved usability and storage stability. Based on these results, SNPs can be a promising alternative platform for the loading of various kinds of enzymes and their broad implementations. The use of such smart nanostructures will show great benefits in improving enzymatic stability, which increases the potential for industrial use of enzymes. It is obvious that the results obtained here will also guide the future development of more advanced transport and delivery systems for the applications of drug/enzyme loaded smart polymeric systems.

**Author Contributions** ÖA: Investigation, Conceptualization, Writing—Review & Editing.

**Data availability** Data will be made available on request.

## Declarations

**Conflicts of interest** There are no conflicts to declare.

## References

- Patel PG, Panseriya HZ, Vala AK, Dave BP, Gosai HB (2022) Process Biochem 121:529
- Noma SAA, Ulu A, Acet Ö, Sanz R, Sanz-Pérez ES, Odabaşı M, Ateş B (2020). New J Chem. <https://doi.org/10.1039/d0nj00127a>
- Ali Noma SA, Acet Ö, Ulu A, Önal B, Odabaşı M, Ateş B (2021) Polym Test 93:106980
- Acet Ö, Aksoy NH, Erdönmez D, Odabaşı M (2018) Artif Cells Nanomed Biotechnol 46:538
- Acet Ö, İnanan T, Acet BÖ, Dikici E, Odabaşı M (2021) Appl Biochem Biotechnol 193:2483
- Rabanel J-M, Banquy X, Zouaoui H, Mokhtar M, Hildgen P (2009) Biotechnol Prog 25:946
- Mohamad NR, Marzuki NHC, Buang NA, Huyop F, Wahab RA (2015) Biotechnol Biotechnol Equip 29:205
- Tran DN, Balkus KJ (2011) ACS Catal 1:956
- da Pereira AS, Souza CPL, Moraes L, Fontes-Sant'Ana GC, Amaral PFF (2021) Polymers (Basel) 13:4061
- Yıldırım M, Acet Ö, Yetkin D, Acet BÖ, Karakoc V, Odabaşı M (2022) J Drug Deliv Sci Technol 74:103552
- Eon-Duval A, Broly H, Gleixner R (2012) Biotechnol Prog 28:608
- Colombo S, Beck-Broichsitter M, Bøtker JP, Malmsten M, Rantanen J, Bohr A (2018) Adv Drug Deliv Rev 128:115
- Brumano LP, da Silva FVS, Costa-Silva TA, Apolinário AC, Santos JHPM, Kleingesinds EK, Monteiro G, de Rangel-Yagui CO, Benyahia B, Junior AP (2019). Front Bioeng Biotechnol. <https://doi.org/10.3389/fbioe.2018.00212>
- Guragain S, Bastakoti BP, Malgras V, Nakashima K, Yamauchi Y (2015) Chem Eur J 21:13164
- Cheng R, Meng F, Deng C, Klok H-A, Zhong Z (2013) Biomaterials 34:3647
- Wu M, Li J, Lin X, Wei Z, Zhang D, Zhao B, Liu X, Liu J (2018) Biomater Sci 6:1457
- Chung JE, Yokoyama M, Yamato M, Aoyagi T, Sakurai Y, Okano T (1999) J Control Release 62:115
- Talenti M, Hennink WE (2011) Nanomedicine 6:1245
- Yan H, Tsujii K (2005) Colloids Surf B 46:142
- Piloni A, Cao C, Garvey CJ, Walther A, Stenzel MH (2019) Macromol Chem Phys 220:1900131
- Asayama S, Sekine T, Kawakami H, Nagaoka S (2007) Nucleic Acids Symp Ser 51:333
- Li Z, Gao Y, Li W, Li Y, Lv H, Zhang D, Peng J, Cheng W, Mei L, Chen H, Zeng X (2022) Smart Mater Med 3:243
- Li Z, Shan X, Chen Z, Gao N, Zeng W, Zeng X, Mei L (2021) Adv Sci 8:2002589
- Acet Ö, Ali Noma SA, Acet BÖ, Dikici E, Osman B, Odabaşı M (2023) J Pharm Biomed Anal 226:115250
- Ulu A, Noma SAA, Koytepe S, Ates B (2019) Appl Biochem Biotechnol 187:938
- Imada A, Igarasi S, Nakahama K, Isono M (1973) J Gen Microbiol 76:85
- Bernfield M, Götte M, Park PW, Reizes O, Fitzgerald ML, Lincecum J, Zako M (1999) Annu Rev Biochem 68:729
- Honary S, Zahir F (2013). Trop J Pharm Res. <https://doi.org/10.4314/tjpr.v12i2.19>
- Cafaggi S, Russo E, Stefani R, Leardi R, Caviglioli G, Parodi B, Bignardi G, de Toterio D, Aiello C, Viale M (2007) J Control Release 121:110
- Yang R, Yang S-G, Shim W-S, Cui F, Cheng G, Kim I-W, Kim D-D, Chung S-J, Shim C-K (2009) J Pharm Sci 98:970
- Noma SAA, Ulu A, Koytepe S, Ateş B (2020) Biocatal Biotransform 38:392
- Noma SAA, Yılmaz BS, Ulu A, Özdemir N, Ateş B (2021) Catal Lett 151:1191
- Gawande PV, Kamat MY (1998) J Biotechnol 66:165
- Monajati M, Borandeh S, Hesami A, Mansouri D, Tamaddon AM (2018) Chem Eng J 354:1153

35. Alam S, Nagpal T, Singhal R, Kumar Khare S (2021) *Bioresour Technol* 339:125599
36. Ulu A, Noma SAA, Koytepe S, Ates B (2018) *Artif Cells Nanomed Biotechnol* 46:1035

**Publisher's Note** Springer Nature remains neutral with regard to jurisdictional claims in published maps and institutional affiliations.

Springer Nature or its licensor (e.g. a society or other partner) holds exclusive rights to this article under a publishing agreement with the author(s) or other rightsholder(s); author self-archiving of the accepted manuscript version of this article is solely governed by the terms of such publishing agreement and applicable law.